

Magnetically Active Stars in Taurus–Auriga: Activity and Rotation

K. N. Grankin

Crimean Astrophysical Observatory, Nauchny, Crimea, 98409 Ukraine

konstantin.grankin@rambler.ru

Abstract

A sample of 70 magnetically active stars toward the Taurus–Auriga star-forming region has been investigated. The positions of the sample stars on the Rossby diagram have been analyzed. All stars are shown to be in the regime of a saturated dynamo, where the X-ray luminosity reaches its maximum and does not depend on the Rossby number. A correlation has been found between the lithium line equivalent width and the age of a solar-mass (from 0.7 to 1.2 M_{\odot}) pre-main-sequence star. The older the age, the smaller the Li line equivalent width. Analysis of the long-term photometric variability of these stars has shown that the photometric activity of the youngest stars is appreciably higher than that of the older objects from the sample. This result can be an indirect confirmation of the evolution of the magnetic field in pre-main-sequence stars from predominantly dipole and axisymmetric to multipole and nonaxisymmetric.

Key words: *stars – physical properties, rotation, activity, pre-main-sequence stars.*

INTRODUCTION

Previously (Grankin 2013b), we investigated a sample of 74 magnetically active stars toward the Taurus–Auriga star-forming region (SFR). The sample contains 24 well-known young pre-main-sequence (PMS) stars and 60 candidates for PMS stars from Wichmann et al. (1996). All sample objects exhibit no optical and near-infrared excesses and, consequently, have no accretion disks. Based on accurate data on their main physical parameters (see Tables 3 and 4 in Grankin 2013a) and published data on their proper motions, X-ray luminosities, and equivalent widths of the $H\alpha$ and Li lines (see Table 1 in Grankin 2013b), we refined the evolutionary status of these objects. As a result, we identified a group of 70 objects with ages 1–40 Myr. We showed that 50 stars from this group belong to the Taurus–Auriga SFR with a high probability. Other 20 objects have a controversial evolutionary status and can belong to both the Taurus–Auriga SFR and the Gould Belt (see Table 3 in Grankin 2013b). For 50 PMS stars with known rotation periods, we analyzed the relationship between their rotation,

mass, and age. The rotation was shown to depend on both mass and age of young stars. We investigated the angular momentum evolution for the sample stars within the first 40 Myr. An active interaction between the sample stars and their protoplanetary disks was shown to have occurred on a time scale from 0.7 to 10 Myr. In this paper, we discuss various magnetic activity parameters for the sample PMS stars and investigate the relationship between their activity and rotation.

ACTIVITY AND ROTATION

All of the PMS stars from our sample exhibit an enhanced variable X-ray emission, which is evidence for the existence of a hot corona and, hence, magnetic activity. The key unsolved question regarding this X-ray emission is whether an analogy exists between the magnetic activity of PMS stars and that of the Sun.

On the Sun and on all of the stars whose internal structure consists of a radiative core and a convective envelope, magnetic activity is probably produced by the so-called $\alpha\Omega$ dynamo mechanism. This mechanism operates in a thin shell lying at the interface between the radiative and convective zones and is generated by the interaction between differential rotation and convective motion (see Schrijver and Zwaan (2000) and references therein). This hypothesis is confirmed by the existence of magnetic activity, which manifests itself through cool photospheric spots, the chromospheric emission in the calcium H and K lines and the $H\alpha$ line, and the coronal X-ray emission. In the long run, this type of dynamo is governed by stellar rotation. As a result, a strong activity–rotation correlation is observed for solar-type stars with ages >100 Myr. This correlation was first found by Skumanich (1972) and was subsequently confirmed by numerous studies (see, e.g., Patten and Simon 1996; Terndrup et al. 2000; Barnes 2001). The correlation usually manifests itself as a linear increase in activity indicators with increasing rotation rate accompanied by activity saturation at a high rotation rate. However, PMS stars are known to be fully convective and, thus, cannot provide a basis for the existence of a solar-type dynamo. As PMS stars evolve toward the main sequence (MS), their rotation rate changes greatly. This can lead to a change in the magnetic field generation mechanisms themselves and, as a consequence, to a change in magnetic activity properties and their relationship to stellar rotation. Thus, investigation of the relationship between magnetic activity and rotation for PMS stars can provide an understanding of the fundamental changes in the physics of stars that occur in the range of ages 1–100 Myr. In the next sections, we will investigate the relationship between the rotation of PMS stars in Taurus–Auriga and various magnetic activity indicators for these stars.

The nature of the relationship between magnetic activity and rotation can be complex, because it depends on the stellar age, mass, internal structure, and, possibly, interaction with the disks at early evolutionary stages. To separate the various processes, we will begin by analyzing the equivalent width of the $H\alpha$ line ($EW(H\alpha)$) as a function of the temperature or spectral type. It should be noted that most of the objects from our sample were identified in X-ray surveys and the sample may be biased toward more active objects. Therefore, when discussing activity, we prefer to use criteria based on the upper limit of activity in our sample and not on the lower limit, because the latter can be shifted greatly.

CHROMOSPHERIC ACTIVITY

The $H\alpha$ line is commonly used as an indicator of chromospheric activity resulting from photoionization and collisions in a hot chromosphere. In Fig. 1, $EW(H\alpha)$ is plotted against

the effective temperature represented by the spectral type in our case. The black and white symbols denote the objects with a reliable and unreliable evolutionary status, respectively (for details, see Grankin 2013b). The objects classified as weak-lined T Tauri stars (WTTS) with ages <10 Myr and as post T Tauri stars (PTTS) with ages >10 Myr are marked by the circles and squares, respectively. It can be seen from the figure that $EW(H\alpha)$ is an obvious function of the spectral type. Whereas the $H\alpha$ line in G-type stars is in absorption ($EW(H\alpha) \sim 2\text{\AA}$), $H\alpha$ in K1–K4 stars exhibits a gradual transition to an emission state. For stars later than K5, $H\alpha$ is always in emission. The scatter of $EW(H\alpha)$ increases and $EW(H\alpha)$ for M-type stars lie within the range from 0 to -7\AA . The dramatic change in $EW(H\alpha)$ with spectral type reflects not only the change in chromospheric activity but also the additional effects related to a reduction in the continuum level with decreasing stellar luminosity and to a change in photospheric absorption in $H\alpha$, which is zero for M dwarfs and increases toward earlier spectral types. The combined effects of a reduction in the continuum level and photospheric absorption in $H\alpha$ were estimated from spectroscopic observations of standard nonactive stars by Scholz et al. (2007). The linear approximation of $EW(H\alpha)$ as a function of the spectral type is indicated in Fig. 1 by the dash-dotted line. This line coincides with the dependence of $EW(H\alpha)$ on spectral type for stars in the Hyades and for field stars of various spectral types (for details, see Scholz et al. 2007). Thus, this line is an estimate for the purely photospheric contribution to $EW(H\alpha)$.

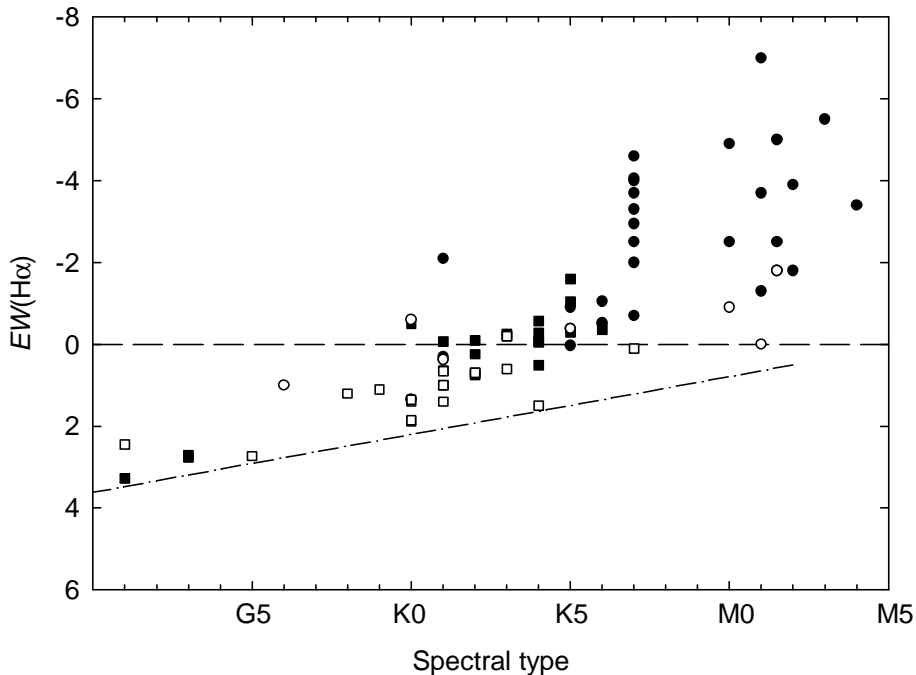


Figure 1: $EW(H\alpha)$ versus spectral type. The dash-dotted line indicates the upper limit of $EW(H\alpha)$ for nonactive field stars. The dashed line corresponds to zero for $EW(H\alpha)$. The black and white symbols denote the objects with a reliable and unreliable evolutionary status, respectively. The objects classified as WTTS (with ages <10 Myr) and PTTS (with ages >10 Myr) are marked by the circles and squares, respectively.

It can be seen from the figure that the dash-dotted line is the lower envelope for the stars of our sample: almost all of the PMS stars in Taurus–Auriga lie above this line, except for seven objects that exhibit no measurable chromospheric activity. Thus, most of the stars from our sample are chromospherically active objects. The maximum activity level increases rapidly for K7–M4 stars.

X-RAY ACTIVITY

First of all, we investigated the possible relationship between the rotation period (P_{rot}) and various X-ray activity parameters of PMS stars: the X-ray luminosity (L_X), the X-ray surface flux (F_X), and the X-ray luminosity excess defined as the X-ray to bolometric luminosity ratio (L_X/L_{bol}). To calculate these X-ray activity parameters, we used data from our two previous papers (Grankin 2013a, 2013b). Figure 2 shows the corresponding graphs on a logarithmic scale. It can be seen from the figure that a very weak correlation is traceable between P_{rot} and L_X (see Fig. 2a). We failed to find any correlation between the rotation period and L_X/L_{bol} (see Fig. 2b). The most significant correlation is observed between P_{rot} and F_X (see Fig. 2c). Nevertheless, it would be unreasonable to assert that there exists an unambiguous correlation between these activity parameters of PMS stars and their rotation period because of the small correlation coefficients.

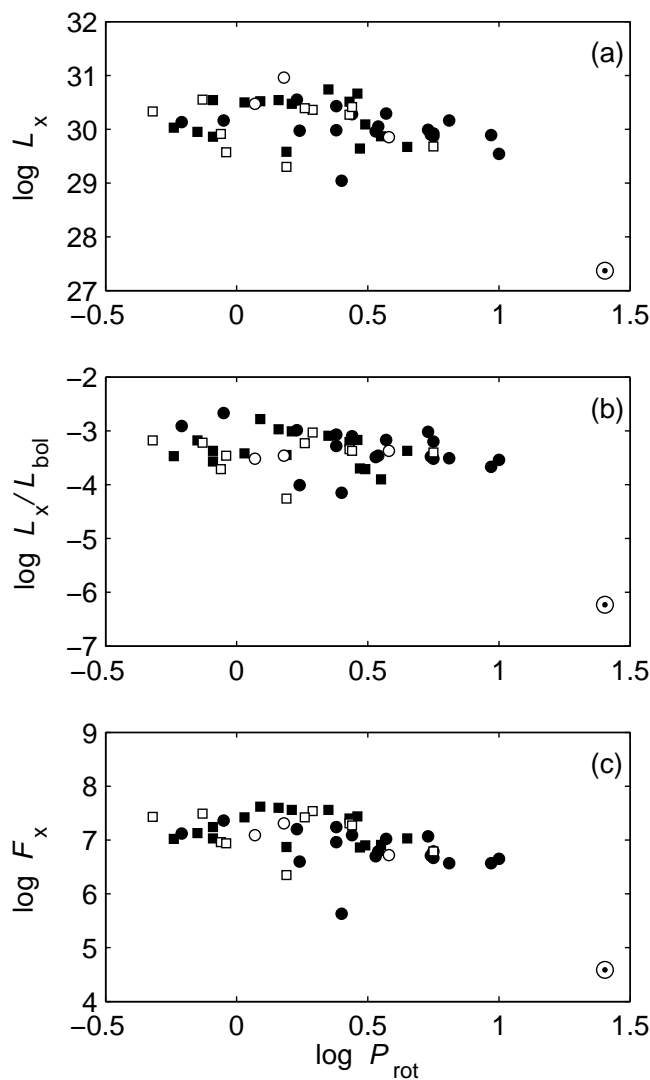


Figure 2: Relationship between rotation period and X-ray activity parameters: the X-ray luminosity L_X (a), the ratio L_X/L_{bol} (b), and the X-ray surface flux F_X (c). The position of the Sun is denoted by the corresponding symbol. The designations of the objects are the same as those in Fig. 1.

We attempted to investigate the possible correlation between the X-ray activity of PMS stars and their angular momentum, which is a no less informative characteristic of stellar rotation.

The angular momentum is $J = I\omega$, where I is the moment of inertia and ω is the angular velocity of the star. The angular velocity of a star is easy to calculate if its rotation period is known: $\omega = 2\pi/P$. The moment of inertia of a star can be determined from the formula $I = M(kR)^2$, where M is the stellar mass, R is the stellar radius, and k is the radius of inertia dependent on the rotation period and shape of the star. Thus, the angular momentum of a star depends on three parameters: its mass, radius, and rotation period. To reduce the number of unknown parameters, we can introduce some normalized angular momentum:

$$j = \frac{J}{M} = \frac{I\omega}{M} = \frac{2\pi M(kR)^2}{MP} = 2\pi k^2 \frac{R^2}{P}.$$

For a spherically symmetric star, $k = \sqrt{2/3}$ and the normalized angular momentum can be calculated from the formula $j = \frac{4\pi}{3} \frac{R^2}{P}$. For the Sun, $P = 25$ days, $R = 6.96 \times 10^{10}$ cm, and the angular momentum $j_{\odot} = 9.39 \times 10^{15} \text{cm}^2 \text{s}^{-1}$.

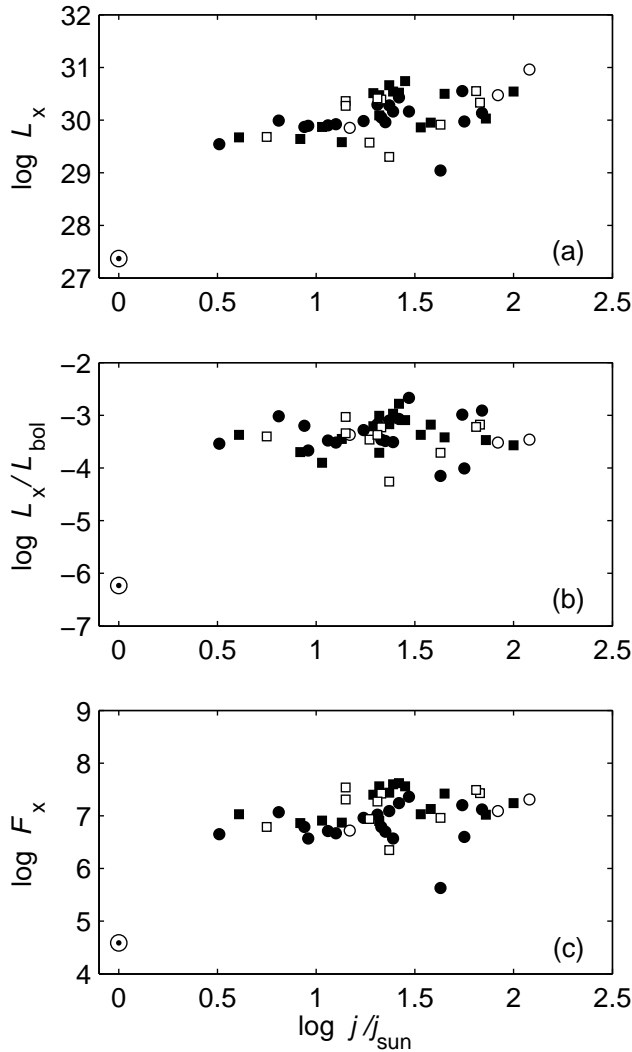


Figure 3: Relationship between angular momentum and various X-ray activity parameters. The sign of the Sun in the lower left corners marks its position. The designations are the same as those in Fig. 1.

We calculated the ratio j/j_{\odot} for all of the stars from our sample with known rotation periods. Based on these data, we plotted the normalized angular momentum (j/j_{\odot}) against

various X-ray activity parameters of PMS stars: L_X (Fig. 3a), L_X/L_{bol} (Fig. 3b), and F_X (Fig. 3c). It can be seen from Fig. 3 that there is no significant correlation between the various X-ray activity parameters and angular momentum, as in the case with the rotation period.

ROSSBY DIAGRAM

The chromospheric and coronal activity of stars is known to be related to their rotation and to the depth of the convective zone or the convective turnover time (τ_c). The existence of such a relationship is in good agreement with qualitative predictions of the $\alpha\Omega$ dynamo theory explaining the generation of a magnetic field. The Rossby diagram is one of the best tools for demonstrating the existence of a relationship between magnetic field generation and stellar activity. As a rule, the Rossby diagram displays the relationship between some stellar activity indicator and the Rossby number (R_0) calculated from the formula $R_0 = P_{\text{rot}}/\tau_c$. In particular, previous studies have shown that the slowly rotating stars in the Hyades cluster and most of the dwarf field stars exhibit a decrease in $\log(L_X/L_{\text{bol}})$ with increasing Rossby number. In contrast, the rapidly rotating field stars and G and K dwarfs in the Pleiades and α Persei clusters exhibit no obvious relationship between $\log(L_X/L_{\text{bol}})$ and the Rossby number (Hempelmann et al. 1995; Patten and Simon 1996; Randich et al. 1996; Queloz et al. 1998). Subsequently, Pizzolato et al. (2003) showed that the relationship between the X-ray luminosity and rotation period of a star could be roughly described by a power law irrespective of its mass and spectral type. Thus, stellar rotation dominates over convection for slowly rotating solar-type stars. At the same time, the X-ray luminosity of rapidly rotating stars depends only on L_{bol} and, consequently, depends on stellar-structure characteristics.

Recent studies have shown that for slowly rotating stars there is a tendency for L_X/L_{bol} to grow with increasing rotation velocity up to $\sim 15 \text{ km s}^{-1}$, while stars with higher velocities have approximately the same L_X/L_{bol} near the saturation level ($L_X/L_{\text{bol}} \sim 10^{-3}$), with this saturation limit being observed for stars in a wide range of spectral types, from G to M. Thus, the most active stars exhibit a maximum X-ray luminosity at a level of $L_X/L_{\text{bol}} \sim 10^{-3}$, which does not depend on the rotation velocity. This phenomenon was called the saturated dynamo effect.

In Fig. 4, $\log(L_X/L_{\text{bol}})$ is plotted against the Rossby number for all of the stars from our sample with known rotation periods. We estimated the convective turnover time τ_c from an empirical relation given in Noyes et al. (1984):

$$\log \tau_c = \begin{cases} 1.362 - 0.166x + 0.025x^2 - 5.323x^3, & x > 0, \\ 1.362 - 0.14x, & x < 0, \end{cases}$$

where $x = 1 - (B - V)$. We used the extinction-corrected color index as $(B - V)$. To compare the activity of PMS stars with the activity of other solar-type stars, we showed the positions of the MS stars and the stars from the Hyades, Pleiades, IC 2391, and IC 2602 open clusters investigated by Pizzolato et al. (2003) in Fig. 4.

It can be seen from Fig. 4 that the X-ray luminosity excess (L_X/L_{bol}) for the sample of active stars from Pizzolato et al. (2003) increases with decreasing Rossby number (R_0). However, the increase in L_X/L_{bol} ceases at a level of about $\log(L_X/L_{\text{bol}}) = -3$, when R_0 reaches $\sim 0.28 - 0.1$ ($\log R_0 = -0.56 - -0.98$). From this time on, the so-called saturation regime is observed, where the X-ray luminosity excess reaches its maximum values and ceases to depend on R_0 .

All PMS stars from our sample exhibit the same L_X/L_{bol} and R_0 as the stars from the IC 2602 and Pleiades open clusters with ages within the range 30–100 Myr. In other words, the X-ray activity of PMS stars in the Taurus–Auriga SFR closely coincides with that of the cluster

stars in the regime of saturated activity. It should be noted that there are slightly more stars with small $\log R_0$ in the range from -1.7 to -2.1 in the Pleiades. Since the stars of our sample are located in the zone of a saturated dynamo, the fact that we failed to find an unequivocal correlation between the rotation period and various X-ray activity parameters (see the previous section) becomes explainable.

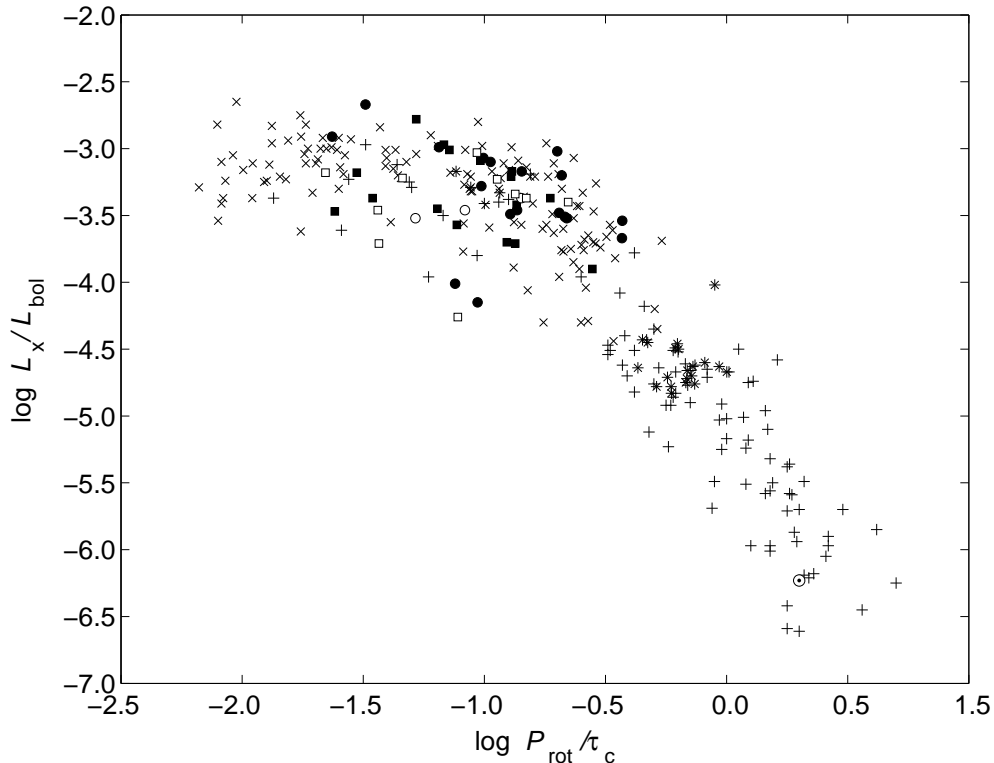


Figure 4: L_X/L_{bol} versus Rossby number. The crosses are stars from the Pleiades, IC 2391, and IC 2602 open clusters; the asterisks are Hyades stars; the pluses are MS dwarfs from Pizzolato et al. (2003). The position of the Sun at the maximum of the activity cycle is also marked. The designations of PMS objects are the same as those in Fig. 1.

PHOTOSPHERIC ACTIVITY

In previous sections, we have pointed out that the magnetic activity of young solar-type stars manifests itself through the chromospheric emission in the calcium H and K lines and the $H\alpha$ line or through the coronal X-ray emission. In addition, the magnetic activity can also manifest itself through the maximum photometric variability amplitude in the optical spectral range (ΔV_{max}). Indeed, the maximum photometric variability amplitude depends primarily on the degree of nonuniformity in the distribution of spotted regions over the stellar surface and, consequently, on the total surface magnetic flux. Before investigating the possible relationship between ΔV_{max} and various rotation parameters, we analyzed the possible correlations of ΔV_{max} with such parameters as the spectral type of a star and its age. In Fig. 5a, the maximum variability amplitude is plotted against the spectral type. It can be seen from the figure that the maximum amplitude gradually increases from earlier spectral types to later ones and reaches its maximum near a spectral type K7–M1. This effect can be due to a change in the contrast of dark spots against the background of the photosphere. The results of modeling this effect are represented by the solid line. It can be clearly seen that the amplitude of the periodicity

increases from relatively early spectral types to later ones. It should be noted that our sample contains five most active WTTS whose maximum amplitudes are considerably larger than those of the remaining PMS stars: LkCa 4, LkCa 7, V827 Tau, V830 Tau, and TAP 41. These stars are separated from the main group by the horizontal dashed line at a level of $0.^m35$. We excluded these objects from the subsequent statistical analysis and will discuss their properties separately.

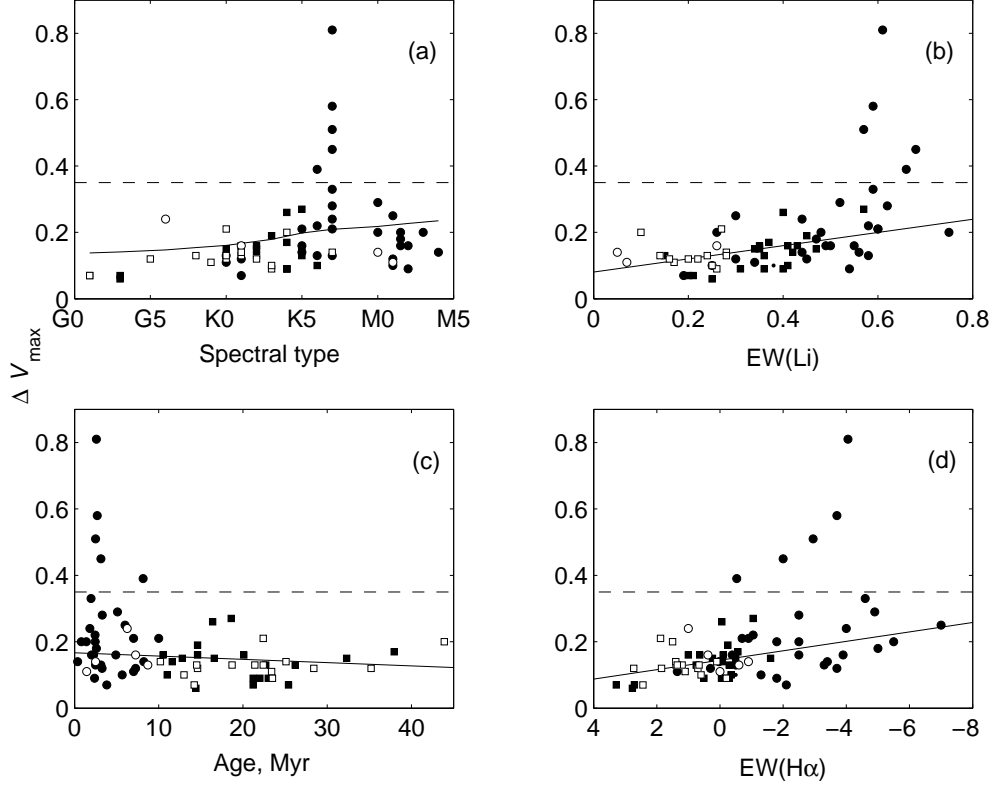


Figure 5: Maximum photometric variability amplitude versus spectral type (a), Li line equivalent width (b), age (c), and H α equivalent width (d). The designations of PMS objects are the same as those in Fig. 1.

In Fig. 5b, ΔV_{\max} is plotted against EW(Li). We found a weak correlation between ΔV_{\max} and EW(Li) with a correlation coefficient $k = 0.39$. The maximum photometric variability amplitude increases with increasing lithium line equivalent width. The existence of such a positive correlation between ΔV_{\max} and EW(Li) may reflect the fact that younger PMS stars are simultaneously also more active objects. For example, it is easy to notice that the five most active WTTS lying above the dashed line have values of EW(Li) that are among the largest ones. This result is quite intriguing, because the presence of a lithium absorption line is considered primarily as a signature of youth and not as a signature of stellar activity.

In Fig. 5c, the maximum photometric variability amplitude is plotted against the age of PMS stars. The solid line is a linear approximation for all of the stars lying below the dashed line ($\Delta V_{\max} < 0.^m35$). A weak correlation between the maximum photometric variability amplitude and age with a correlation coefficient $k = 0.45$ is noticeable. The maximum amplitude decreases with increasing stellar age. The four stars exhibiting the largest variability amplitudes and lying above the horizontal dashed line have ages 2.5 – 3.1 Myr.

In Fig. 5d, ΔV_{\max} is plotted against EW(H α). The solid line is a linear approximation for all of the stars lying below the horizontal dashed line ($\Delta V_{\max} < 0.^m35$). It can be seen from the figure that there is a clear correlation between ΔV_{\max} and EW(H α) with a correlation

coefficient $k = 0.46$. As the $H\alpha$ line passes from an absorption state to an emission one, the maximum photometric variability amplitude increases monotonically. This result confirms our assumption that the maximum photometric variability amplitude can be used as an indicator of photospheric activity, while the $H\alpha$ line is an indicator of chromospheric activity for PMS stars.

In the previous section, we showed that the PMS stars in Taurus–Auriga are in the regime of a saturated dynamo, where the X-ray flux reaches saturation and ceases to depend on the rotation rate. Since the X-ray flux is related to the number of active regions on the stellar surface, we can assume that the active regions should cover almost the entire stellar surface in the regime of a saturated dynamo. In that case, we may expect maximum photometric variability amplitudes for PMS stars, of course, only when the active regions are distributed over the stellar surface highly nonuniformly. Therefore, it is interesting to investigate the relationship between ΔV_{\max} and such stellar rotation parameters as the rotation period, the Rossby number, the equatorial rotation velocity, and the angular momentum. For this purpose, we constructed the corresponding dependences but failed to find a clear correlation between ΔV_{\max} and the rotation parameters listed above. This result confirms our conclusion that the PMS stars are in a state of saturated dynamo. Regarding the five most active stars that exhibit the largest variability amplitudes ($\Delta V_{\max} > 0.^m35$), it should be noted that they have moderate rotation velocities ($v_{\text{eq}} = 10 - 30 \text{ km s}^{-1}$) and are in the region of the transition into the zone of a saturated dynamo that corresponds to Rossby numbers in the range $\log(P_{\text{rot}}/\tau_c) = -0.56 - -0.98$.

Li EVOLUTION DURING THE PMS STAGE

Lithium, just as other light elements, such as beryllium and boron, is burnt out in thermonuclear reactions at relatively low temperatures in the stellar interior ($(2.5 - 3.0) \times 10^6 \text{ K}$). In the case of initial evolution of low-mass ($M < 1.2 M_{\odot}$) stars, efficient mixing can rapidly transport a lithium-depleted material from the central regions of a PMS star to its photosphere. For this reason, measurements of the photospheric Li abundance provide one of the few means for probing the stellar interior and are a sensitive test of evolution models for PMS stars. Understanding the Li depletion mechanisms at the stage of PMS stars also makes it possible to estimate the ages of young stars.

A large number of observational and theoretical works were devoted to understanding the initial abundance of Li and its subsequent PMS evolution (see the recent review by Jeffries 2006). According to classical models, the photospheric depletion of Li begins near 2 Myr for a star with a mass of $1 M_{\odot}$ and should end in an age of about 15 Myr. This window moves toward older ages for stars with lower masses. However, the degree of Li depletion depends very strongly on mass, convection efficiency, opacity, metallicity, and other model parameters. Thus, the amount of photospheric Li can serve as a characteristic of the youth of a PMS star. Nevertheless, numerous observations of the photospheric lithium abundance in hundreds of young stars in open clusters suggest that the degree of Li depletion in these stars is considerably smaller than what is predicted by standard models. In addition, the K-type stars in clusters with ages of less than 250 Myr are characterized by a significant dispersion in Li abundance whose cause is not yet completely understood (Jeffries 2006).

This and other puzzling peculiarities that are unexpected within the framework of standard models suggest that Li depletion is governed not only by convection and that there exist other, unknown processes that have not been included in the classical theory. In recent years, several nonstandard models explaining the physics of the possible processes leading to Li depletion

have been proposed. However, the mechanisms governing Li depletion still remain poorly studied. Additional observational constraints for present-day models are badly needed for further progress in understanding the evolution of Li during the PMS stage.

That is why we attempted to reveal any correlations or relationships between the Li equivalent width and other physical parameters of the PMS stars from our sample. Finding such correlations can shed light on the problem of Li depletion at the PMS evolutionary phase of young stars. In the previous section, we pointed out that there exists a weak positive correlation between $\text{EW}(\text{Li})$ and ΔV_{max} for PMS stars. At the same time, we failed to find any correlation between $\text{EW}(\text{Li})$ and the X-ray luminosity.

Below, we investigate the possible correlation between $\text{EW}(\text{Li})$ and such parameters of PMS stars as the theoretical age (t) and the rotation period (P_{rot}).

If the entire sample of stars is considered as a single group, then no correlation is observed between $\text{EW}(\text{Li})$ and t . It should be noted that our sample includes PMS stars with quite different physical parameters. For example, the masses of the PMS stars from our sample lie within the range $0.26 - 2.2 M_{\odot}$. Since the degree of Li depletion depends very strongly on mass, we attempted to find a possible correlation between $\text{EW}(\text{Li})$, age, and rotation period for stars with masses fairly close to the solar mass (in the range $0.7 - 1.2 M_{\odot}$). In Fig. 6, $\text{EW}(\text{Li})$ is plotted against t (a) and P_{rot} (b).

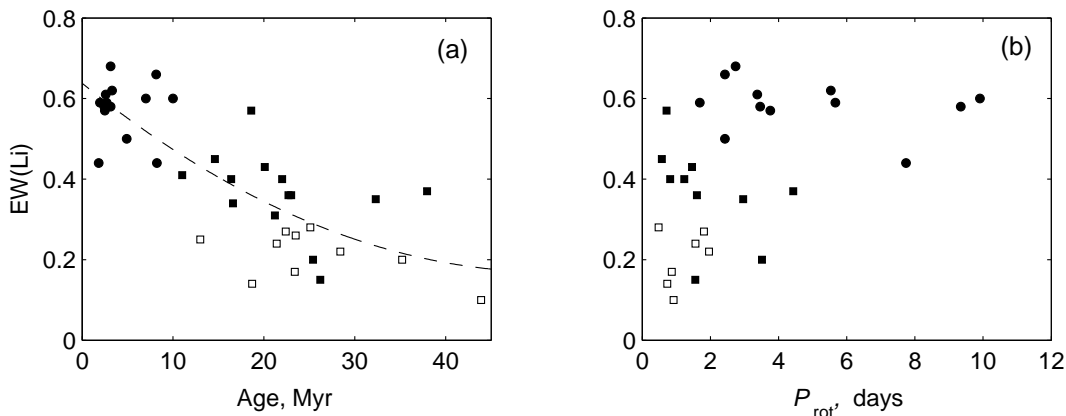


Figure 6: $\text{EW}(\text{Li})$ versus age (a) and rotation period (b). The designations are the same as those in Fig. 1.

For solar-mass stars, there exists a statistically significant correlation between $\text{EW}(\text{Li})$ and t with a correlation coefficient of 0.68. The older the age, the smaller the equivalent width $\text{EW}(\text{Li})$. The stars with ages $\sim 2 - 3$ Myr have maximum values of $\text{EW}(\text{Li})$ ($\sim 0.58 \text{ \AA}$). In contrast, the stars with ages older than 30 Myr exhibit minimum values of $\text{EW}(\text{Li})$ (about 0.20 \AA). This result is in excellent agreement with the predictions of the classical models explaining the evolution of the atmospheric Li abundance during the PMS evolutionary stage of solar-mass stars.

If the entire sample of stars is considered as a single group, then no correlation is observed between $\text{EW}(\text{Li})$ and P_{rot} . It can also be noted that the stars with rotation periods longer than 5 days have relatively broad Li absorption lines ($\text{EW}(\text{Li}) > 0.4 \text{ \AA}$). In contrast, the stars with periods shorter than 5 days have various values of $\text{EW}(\text{Li})$, from 0.2 to 0.7 \AA . If each subgroup of stars is considered separately, then the following can be identified: (1) the reliable WTTS (black circles) have $\text{EW}(\text{Li}) \sim 0.6 \text{ \AA}$ for the entire range of rotation periods from 0.5 to 10 days; (2) the reliable PTTS (black squares) with ages older than 10 Myr have $\text{EW}(\text{Li}) \sim 0.4 \text{ \AA}$ for their range of rotation periods from 0.5 to 5 days; (3) the PTTS with an unreliable evolutionary

status rotate more rapidly (P_{rot} in the range from 0.5 to 2 days) and have $\text{EW}(\text{Li}) \sim 0.2 \text{ \AA}$. In other words, the same dependence of the lithium line equivalent width on age, but not on rotation period, is observed.

PROPERTIES OF THE MOST ACTIVE PMS STARS

Several most active stars that exhibit the record maximum photometric variability amplitudes deserve particular attention: LkCa 4 ($0^m.81$), LkCa 7 ($0^m.58$), V827 Tau [TAP 42] ($0^m.51$), V830 Tau ($0^m.45$), and V1075 Tau [TAP 41] ($0^m.39$). It should be noted that there are two more objects that exhibit large variability amplitudes: V410 Tau ($0^m.63$) and V836 Tau ($0^m.62$). However, we do not discuss their properties here, because we failed to determine reliable luminosities, radii, masses, and ages for them. Such large amplitudes of light variations can be due to the existence of very large and extended spotted regions in the photospheres of these stars; these extended spotted regions must be distributed over the surface highly nonuniformly, otherwise the very large amplitudes of periodic light variations reaching $0^m.4 - 0^m.8$ cannot be explained.

A previous analysis of long-term photometric observations for a sample of well-known WTTS from the Taurus–Auriga SFR showed that some of these objects exhibit stability of the phase of minimum light (φ_{min}) over several years of observations (see, e.g., Grankin et al. (2008) and references therein). Only seven stars from the entire sample of known WTTS show stability of φ_{min} in the interval from 5 to 19 years: LkCa 4, LkCa 7, V819 Tau, V827 Tau, V830 Tau, V836 Tau, and V410 Tau. Such long-term stability of φ_{min} can be due to the existence of the so-called active longitudes at which short-lived groups of spots are located (Grankin et al. 1995). Similar long-lived active regions are known on the Sun and some of the RS CVn binary stars.

It should be noted that almost all of these stars enter into the list of seven most active objects that exhibit the largest photometric variability amplitudes (see above). Thus, the stability of the phase of minimum light for these objects is somehow related to the existence of very large variability amplitudes. Given the unusual photometric properties of these active stars, we decided to discuss their main physical parameters in more detail.

First, all of the most active stars with known parameters have very similar spectral types in the range K6–K7 and, hence, almost identical surface temperatures. Second, the rotation periods of these active stars lie within a fairly narrow range, from 2.4 to 5.7 days. Third, the radii of these stars are fairly close and lie within the range from 1.30 to $1.75 R_{\odot}$. Fourth, analysis of their positions on the Hertzsprung–Russell diagram showed that their masses also have close values (from 0.74 to $0.92 M_{\odot}$), while their ages lie within the range from 2.5 to 8.2 Myr.

Apart from the similarity of the main parameters of these stars noted above, it should be noted that they exhibit the broadest lithium lines with $\text{EW}(\text{Li}) > 0.57 \text{ \AA}$. This fact confirms our assumption that the lithium line equivalent width can be used as an activity and youth criterion for stars, because there exists a significant correlation between $\text{EW}(\text{Li})$, the mean photometric variability amplitude, and the age of PMS stars (see Figs. 5b and 6a).

We limited our sample of stars in mass and considered only those objects whose masses were close to the solar mass (within the range from 0.7 to $1.2 M_{\odot}$). In this case, all five most active stars exhibit the strongest $\text{H}\alpha$ emission lines and are among the youngest ones, with ages from 2.5 to 3 Myr, except TAP 41 whose age is estimated to be 8 Myr.

Thus, if the subgroup of solar-mass PMS stars is considered, then it can be asserted that the most active and youngest stars with ages of no more than 8 Myr have the largest photometric

variability amplitudes (reaching $0^m.39 - 0^m.81$), show H α emission in the range from -0.5 to -4.0 \AA , and exhibit the most stable phase light curves and the strongest lithium absorption line ($\text{EW}(\text{Li}) > 0.57 \text{ \AA}$).

EVOLUTION OF THE PHASE LIGHT CURVES

The evolution of the phase light curves for the most active PMS stars was analyzed in detail by Grankin et al. (2008). Here, we will point out the most interesting results. Despite the stability of the phase light curves in the sense of stability of the phase of minimum light, all active stars exhibit significant changes in the amplitude and shape of the phase light curve from season to season. For example, the amplitude for LkCa 7 changes from $0^m.33$ to $0^m.58$. The most symmetric (relative to φ_{\min}) phase light curve, as a rule, corresponds to the season with a maximum amplitude. Conversely, the most asymmetric phase light curves correspond to minimum amplitudes of light variations.

Whereas many of the stars show gradual changes in the amplitude and shape of the light curve from season to season (for example, LkCa 4 and LkCa 7), there are examples of a completely different behavior. The amplitude of periodic light variations can change noticeably by a few tenths of a magnitude during one season, as in the case of TAP 41.

Although the amplitude of the light curve can change noticeably, the mean brightness level is essentially constant. Simple simulations showed that the stability of the mean brightness level from season to season suggests that the total number of spots on the surfaces of active stars changes much less than their distribution over the stellar surface. In other words, the decrease in the amplitude of the periodicity is attributable not to a decrease in the total area of the spots (in this case, the mean brightness level should increase) but to a more uniform distribution of the spots over the stellar surface. However, it should be noted that some of the stars exhibit noticeable changes in the mean brightness level from season to season (V819 Tau, V827 Tau, V836 Tau, and VY Tau).

All the noted peculiarities of the evolution of the phase light curves concerned the most active and youngest stars of our sample. However, the overwhelming majority of sample stars show a slightly different photometric behavior that was not discussed in previous papers. In particular, many of the PMS stars exhibit modest variability amplitudes that do not exceed $0^m.1 - 0^m.2$. In addition, periodic light variations are observed much more rarely than in the most active PMS stars whose properties have been discussed above. The differences in photometric behavior between the most active PMS stars and the remaining sample stars are presented in Fig. 7. Figures 7a and 7b show the seasonal phase light curves, respectively, for V819 Tau, one of the most active and youngest WTTS with an age of 3.3 Myr, and for W62 (RXJ0452.5+1730), a reliable PTTS with an age of 22 Myr. It can be seen from the figure that clear periodic light variations in W62 were detected only in two of the six seasons: in 2001 and 2004. In contrast, periodic light variations in V819 Tau were observed during each observing season. The phase of minimum light remained stable over 6 years (from 1999 to 2004).

To quantitatively characterize the frequency of occurrence of a periodicity, we used a simple parameter, $f = N_p/N_s$, where N_p is the number of observing seasons with periodic light variations and N_s is the total number of observing seasons (see Grankin 2013a). For example, the most active PMS stars exhibit periodic light variations virtually during each observing season, i.e., the frequency of occurrence of a periodicity is $f = 1$.

The less active PMS stars show periodic light variations with a mean frequency ~ 0.5 , i.e., periodic light variations were detected in half of the observing seasons. Since most of the stars from our sample are not so young and active, we investigated the relationship between the

frequency of occurrence of a periodicity and such parameters of PMS stars as $EW(Li)$ (Fig. 8a) and the age (Fig. 8b). It can be seen from Fig. 8a that the frequency of occurrence of a periodicity increases with increasing $EW(Li)$. The dependence of f on age (Fig. 8b) shows that the frequency of occurrence of a periodicity is at a maximum for the youngest stars and gradually decreases for older objects.

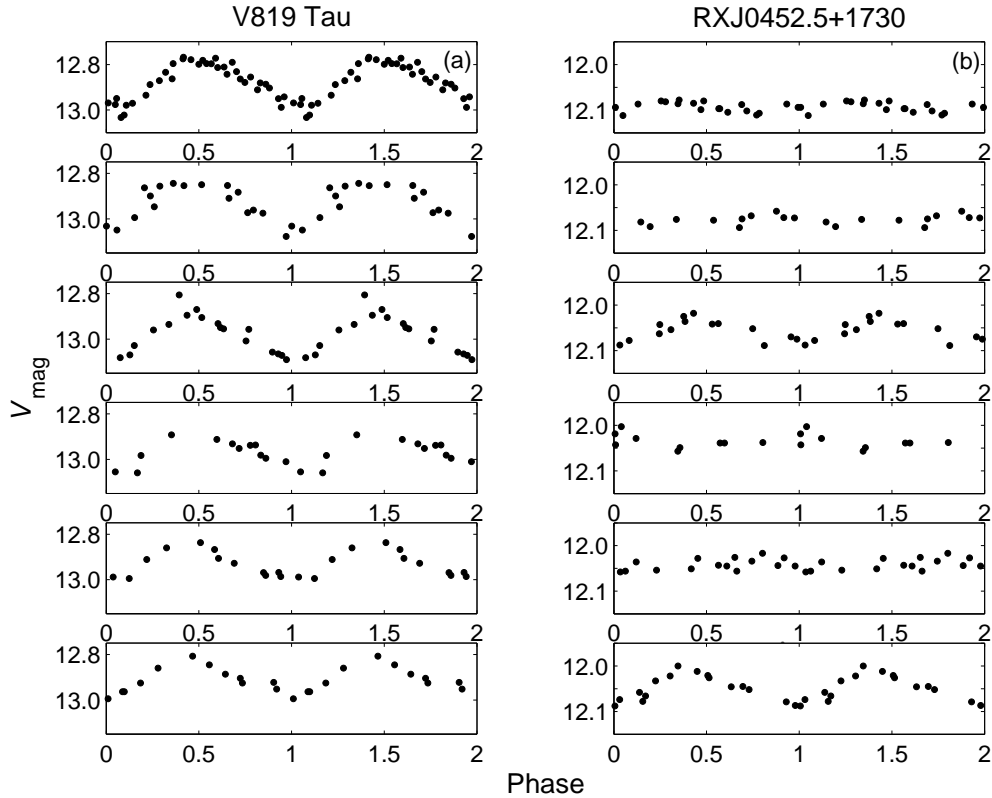


Figure 7: Phase light curves over six years of observations (from 1999 to 2004) for V819 Tau with an age of 3.3 Myr (a) and for W62 (RXJ0452.5+1730) with an age of 22 Myr (b).

In our previous papers, we showed that a small periodicity amplitude suggests a more uniform distribution of spots over the stellar surface, while a large amplitude is typical of the case where the spots are concentrated in one or two high-latitude regions, i.e., they are distributed highly nonuniformly (see Grankin 1999; Grankin et al. 2008). These conclusions are confirmed by the Doppler mapping of the surfaces of selected PMS stars. In particular, cool long-lived high-latitude spots were shown to have dominated on the surface of V410 Tau in the period 1992–1993, when the photometric variability amplitude was at a maximum and reached $0^m.5 - 0^m.6$ (Rice and Strassmeier 1996). In contrast, in the period 2007–2009, when the photometric variability amplitude decreased to $0^m.06 - 0^m.10$ (Grankin and Artemenko 2009), Doppler mapping showed that quite a few low-latitude spots distributed in longitude almost uniformly were present on the stellar surface (see Fig. 4 in Skelly et al. 2010). Thus, it can be assumed that the above differences in photometric behavior between the youngest PMS stars and older sample objects are attributable to different patterns of distribution of the spots over the stellar surface. Since the positions of cool magnetic spots on the surfaces of stars with convective envelopes are related to the locations of local magnetic fields, it is obvious that the pattern of distribution of the spots over the surface will depend on the magnetic field structure. Since the photometric behavior of the most active and youngest objects suggests that long-lived spots are concentrated at high latitudes, it can be assumed that the magnetic field of these

stars has a simpler and fairly symmetric dipole structure. Owing to such a structure, the spots are concentrated predominantly near the magnetic poles and retain their positions during many rotation cycles. It is such a behavior that we observe in the case of the most active and youngest objects. In contrast, the relatively old stars can have a more complex magnetic field structure. Therefore, the spots are distributed over the surface more uniformly; the amplitude of the periodicity is much smaller or it is not observed at all. Such a photometric behavior is typical of the older objects from our sample. In other words, the existence of a correlation between the photometric behavior and age can be a consequence of the evolution of the magnetic field structure for PMS stars.

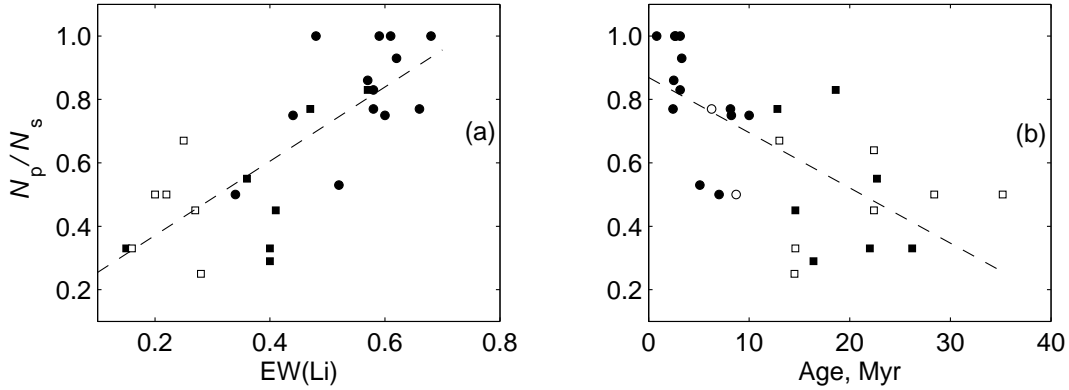


Figure 8: Frequency of occurrence of a periodicity $f = N_p/N_s$ versus lithium line equivalent width (a) and age (b).

This assumption is in good agreement with the results of a recent study of the magnetic field topology for several PMS stars performed within the MaPP (Magnetic Protostars and Planets) Program (see, e.g., Donati et al. (2010, 2011) and references therein). In particular, these studies showed that the magnetic field structure evolves from predominantly dipole and axisymmetric (in the case of fully convective stars) to octupole and axisymmetric (when the radiative core is less than half the stellar radius) and then to multipole and nonaxisymmetric (when the convective zone occupies less than half the stellar radius). The fact that the five most active stars discussed above lie on the Hertzsprung–Russell diagram in the region where fully convective PMS stars with a predominantly dipole and axisymmetric magnetic field structure are located can serve as an additional argument for such evolution of the magnetic field. Our future cooperative studies of the magnetic field topology for 40 PMS stars planned as part of the MaTYSSE (Magnetic Topologies of Young Stars & the Survival of close-in massive Exoplanets) Program performed on TBL (NARVAL spectrograph) and CFHT (ESPaDOnS spectrograph) will show whether the changes in the amplitude of the light curve are accompanied by significant changes in the distribution of spots and/or magnetic field topology.

CONCLUSIONS

We analyzed a sample of 70 magnetically active stars toward the Taurus–Auriga SFR and investigated the relationship between magnetic activity and rotation for these objects. In particular, we obtained the following results.

We analyzed the relationship between various X-ray activity parameters and rotation for PMS stars in the Taurus–Auriga SFR. We showed that there is no significant correlation between various X-ray activity parameters (L_X , L_X/L_{bol} , and F_X) and rotation parameters, such

as the period and the angular momentum. We investigated the positions of PMS stars on the Rossby diagram. All sample stars exhibit the same L_X/L_{bol} and R_0 as the stars from the Pleiades and IC 2602 clusters with ages within the range 30 – 100 Myr, i.e., they are in the regime of a saturated dynamo.

We analyzed the photospheric activity of PMS stars based on original long-term photometric observations. The maximum photometric variability amplitude was found, on average, to decrease with increasing age of the sample objects and to increase with increasing equivalent width of the H α emission line and the lithium absorption line.

We found a statistically significant correlation between the lithium line equivalent width and the age of solar-mass (in the range from 0.7 to 1.2 M_\odot) PMS stars. The older the age, the smaller the Li line equivalent width. This result is in excellent agreement with the predictions of the classical models explaining the evolution of the atmospheric Li abundance during the PMS stage of evolution of solar-mass stars.

We identified a group of five most active PMS stars that exhibit maximum photometric variability amplitudes reaching $0.^m4 - 0.^m8$. All these stars have very similar physical parameters: spectral types (K6–K7), rotation periods (2.4–5.7 days), radii (1.3–1.75 R_\odot), masses (0.74–0.92 M_\odot), and ages (2.5–8.2 Myr). In addition, they show a prominent emission in H α (from -0.5 \AA to -4.0 \AA) and the strongest lithium absorption line ($\text{EW}(\text{Li}) > 0.57 \text{ \AA}$).

The most interesting feature of the photometric behavior of these active stars is related to the stability of the phase light curve over several observing seasons. The long-term stability of the phase light curves manifests itself in the fact that the phase of minimum light (φ_{min}) retains its value in the interval from 5 to 19 years. Such a feature of the photometric behavior may be attributable to peculiarities of the magnetic field configuration for these stars. The most active and youngest stars from our sample most likely have mainly large-scale magnetic fields with an axisymmetric poloidal configuration. In this case, extended spotted regions are concentrated near the locations of two magnetic poles. The long existence of extended spotted regions suggests that the structure of these dipole fields is fairly stable over several years.

The remaining sample stars exhibit small photometric variability amplitudes (no more than $0.^m15$), with a periodicity being observed not in each observing season. The frequency of occurrence of a periodicity was shown to be maximal for the youngest stars and to gradually decrease for older objects. It may well be that the existence of this relationship is an indirect confirmation of the evolution of the magnetic field structure for young stars from predominantly dipole and axisymmetric (in the case of fully convective stars) to octupole and axisymmetric (when the radiative core is less than half the stellar radius) and then to multipole and non-axisymmetric (when the convective zone occupies less than half the stellar radius). The fact that the five most active stars lie on the Hertzsprung–Russell diagram in the region where fully convective PMS stars with a fairly simple dipolar magnetic field structure are located can serve as an additional argument for such evolution of the magnetic field.

REFERENCES

1. S.A. Barnes, *Astrophys. J.* **561**, 1095 (2001).
2. J.-F. Donati, M.B. Skelly, J. Bouvier, et al., *Mon. Not. R. Astron. Soc.* **409**, 1347 (2010).
3. J.-F. Donati, J. Bouvier, F.M. Walter, et al., *Mon. Not. R. Astron. Soc.* **412**, 2454 (2011).
4. K.N. Grankin, *Astron. Lett.* **25**, 526 (1999).

5. K.N. Grankin and S.A. Artemenko, *Inform. Bull. Var. Stars*, 5907 (2009).
6. K.N. Grankin, *Astron. Lett.* **39**, 251 (2013a).
7. K.N. Grankin, *Astron. Lett.* **39**, 336 (2013b).
8. K.N. Grankin, J. Bouvier, W. Herbst, et al., *Astron. Astrophys.* **479**, 827 (2008).
9. K. N. Grankin, M. A. Ibragimov, V. B. Kondrat'ev, et al., *Astron. Rep.* **39**, 799 (1995).
10. A. Hempelmann, J.H.M.M. Schmitt, M. Schultz, et al., *Astron. Astrophys.* **294**, 515 (1995).
11. R.D. Jeffries, in *Chemical Abundances and Mixing in Stars in the Milky Way and its Satellites*, Ed. by S. Randich and L. Pasquini (Springer, Berlin, 2006), p. 163.
12. R.W. Noyes, L.W. Hartmann, S.L. Baliunas, et al., *Astrophys. J.* **279**, 763 (1984).
13. B.M. Patten and T. Simon, *Astrophys. J. Suppl. Ser.* **106**, 489 (1996).
14. N. Pizzolato, A. Maggio, G. Micela, et al., *Astron. Astrophys.* **397**, 147 (2003).
15. D. Queloz, S. Allain, J.-C. Mermilliod, et al., *Astron. Astrophys.* **335**, 183 (1998).
16. S. Randich, J.H.M.M. Schmitt, C.F. Prosser, et al., *Astron. Astrophys.* **305**, 785 (1996).
17. J.B. Rice and K.G. Strassmeier, *Astron. Astrophys.* **316**, 164 (1996).
18. A. Scholz, J. Coffey, A. Brandeker, et al., *Astrophys. J.* **662**, 1254 (2007).
19. C. J. Schrijver and C. Zwaan, *Solar and Stellar Magnetic Activity* (Cambridge Univ. Press, Cambridge, 2000).
20. M.B. Skelly, J.-F. Donati, J. Bouvier, K.N. Grankin, et al., *Mon. Not. R. Astron. Soc.* **403**, 159 (2010).
21. A. Skumanich, *Astrophys. J.* **171**, 565 (1972).
22. D.M. Terndrup, J.R. Stauffer, M.H. Pinsonneault, et al., *Astron. J.* **119**, 1303 (2000).
23. R. Wichmann, J. Krautter, J.H.M.M. Schmitt, et al., *Astron. Astrophys.* **312**, 439 (1996).